International Journal of Nanoelectronics and Materials
IJNeaM
ISSN 1985-5761 | E-ISSN 2232-1535

The performance of epoxy/boron nitrade/cordierite underfill materials: single system

Huai Man Ooi[a] , Pei Leng Teh [a,b]*, Cheow Keat Yeoh[a,b], Mohd Fairul Sharin Abdul Razak[a], Mohd Hanif Mohd Pisal[a], Chun Hong Voon[c], Nor Azura Abdul Rahim[a], Mohamad Nur Fuadi Bin Pargi[d], Halimatuddahliana Nadutionand[e], Mohamad Syahmie Mohamad Rasidi[a] and Bee Ying Lim[a]

[a]*Faculty of Chemical Engineering Technology, Universiti Malaysia Perlis, Kompleks Pusat Pengajian Jejawi 2, Taman Muhibbah, Perlis, Arau, 02600, Malaysia.*
[b]*Frontier Materials Research, Centre of Excellence (FrontMate), Universiti Malaysia Perlis, Lot 106, 108 & 110, Blok A, Taman Pertiwi Indah, Jalan Kangar-Alor Setar, Seriab, Perlis, Kangar, 01000, Malaysia.*
[c]*Institute of Nano Electronic Engineering, Universiti Malaysia Perlis, Lot 106, 108 & 110, Blok A, Taman Pertiwi Indah, Jalan Kangar-Alor Setar, Seriab, Perlis, Kangar, 01000, Malaysia.*
[d]*Faculty of Innovative Design and Technology, Universiti Sultan Zainal Abidin, Kampus Gong Badak, Kuala Nerus, Terengganu Darul Iman, 21300, Malaysia.*
[e]*Department of Chemical Engineering, Faculty of Engineering, Universitas Sumatera Utara,Padang Bulan, Medan 20155, Indonesia.*
**Corresponding author: Pei Leng Teh; e-mail: plteh@unimap.edu.my*

Received 10 May 2026, Revised 25 May 2026, Accepted 5 June 2026

ABSTRACT

This study focuses on optimizing single filler systems for hexagonal boron nitride (hBN) and cordierite (COR) to evaluate their distinct impacts on the performance of epoxy underfill materials in microelectronic packaging. Epoxy's thermal conductivity is a constraint to the epoxy's heat dissipation at high power densities. Furthermore, high filler loadings often hinder the mechanical integrity of epoxy and the processability of epoxy underfills for microelectronics. This study investigates the balance between processing constraints and functional improvements by analysing the effects of filler loadings. The study aims to manage the trade-offs among thermal conductivity, glass transition temperature, coefficient of thermal expansion, and rheological behavior, as well as form the structural and electrical integrity of the underfills, through their mechanical strength and dielectric properties. The study examines the surface interactions of the fillers, the physical appearance of the fillers, and their surface chemistries, as they impact the epoxy and dictate the fillers' dispersion and the interfacial bonding between the fillers and the epoxy matrix. The information the study considers affects the performance of the fillers and is a metric for the performance of underfills in a targeted design of specialized semiconductors.

Keywords: *Epoxy underfill, Boron nitride, Cordierite, Thermal conductivity, Dielectric properties*

1. INTRODUCTION

Underfill materials used in modern package topologies must meet strict reliability criteria due to the continuous trend in microelectronics toward higher powerful densities and smaller form factors. Although epoxy-based underfills are preferred due to their robust adhesion and processing flexibility, providing reliable processing and effective heat dissipation remains a challenge. The poor intrinsic thermal conductivity of epoxy underfills usually limits their capacity to control heat in high-power devices [1]. To create efficient heat pathways within the epoxy matrix while maintaining electrical insulation and dielectric stability, a significant amount of research has concentrated on adding thermally conductive fillers [1-3].

In this context, single fillers such as cordierite (C) and boron nitride (BN) offer unique performance advantages. Because of BN's well-known high in-plane thermal conductivity and superior electrical insulation, BN-filled epoxies represent an advanced approach to improving thermal transport without sacrificing dielectric integrity, provided that dispersion is carefully managed [1,2,4].

On the other hand, when matched with device substrates, the intrinsically low coefficient of thermal expansion (CTE) and the dielectric stability of cordierite can help minimize the thermo-mechanical stress at solder joints. However, the cordierite alone often requires careful microstructural design and dispersion in the polymer matrix to provide meaningful thermal conduction [5-7].

The systematic review indicates the impact of filler content variation on the viscosity and processability, mechanical strength and stiffness, thermal characteristics, and dielectric behavior of both BN and cordierite fillers. The formation of percolation networks for thermal conduction, low dielectric loss retention, and stable Tg are all controlled by the dispersion conditions and the interfacial interactions between the filler and epoxy. To take advantage of cordierite's low coefficient of thermal expansion (CTE) and dielectric benefits without suffering from high viscosity or processing issues, a uniform dispersion of cordierite is needed, but morphological investigations show that BN can be freely dispersed to

create effective thermal networks with minimal resistance to movement of the polymer [1-7].

These observations form a fundamental performance profile for single filler underfills and provide the basis for developing advanced epoxy underfills tailored to high-power-density semiconductor applications. The challenge in these applications is to achieve an optimal balance between thermal management, processing efficiencies, and long-term reliability.

1.1. Theoretical Background

Epoxy resin is a thermoset made of diglycidyl ether of bisphenol A (DGEBA). It produces a three-dimensional network through crosslinking with curing agents. In crosslinked epoxy polymers, the glass transition temperature (Tg) and stiffness of the network polymer are positively correlated with the crosslink density. With the reduction of network density, the glass transition temperature (Tg) decreases, and the toughness and heat resistance of the polymer network are negatively impacted [8, 9].

Neat epoxy in microelectronics provides excellent adhesion, good electric insulation and good stability but high coefficient of thermal expansion (CTE) and low intrinsic thermal conductivity about 0.2 W/mK. The use of epoxy resin and its composites in electronics requires the addition of fillers to the epoxy resin to obtain desired thermal and mechanical properties to improve the reliability of the electronic device to thermal cycling and solder-joint fatigue [10, 11]. Filler strategies aim to balance processability and dielectric performance for high-frequency operations [12 - 14].

Hexagonal boron nitride (hBN) or white graphite is a material with high intrinsic thermal conductivity and electrical resistance, which makes it an ideal filler for epoxy-based underfills in microelectronics products. The plate-like morphology of hBN is responsible for the highly anisotropic and phonon-dominant heat conduction. The in-plane thermal conductivity of hBN is more than an order of magnitude higher than the through-plane value due to the layered structure and the weak interlayer van der Waals interactions [15–17]. The heat conduction pathways in the hBN-embedded epoxy matrix can be converted from distributed platelets to continuous pathways by a percolated network, which reduces the thermal resistance. The percolation threshold is influenced by the filler content, aspect ratio, orientation, and dispersion quality [15,18,19]. Beyond the threshold, the viscosity will increase, which may be detrimental to the capillary filling during underfill processing. Therefore, practical implementation requires processing methods that promote network development while preserving flow [20-22].

Several design solutions have been developed to reduce anisotropy and optimize network development at realistic loadings. Isotropic choices aim to maintain balanced conductivity in all directions, but orientation control, for instance, can increase through-plane conduction when fillers are aligned to generate quasi-2D conductive pathways. The importance of filler orientation in modulating thermophysical properties is highlighted by the fact that magnetic alignment of hBN platelets has been shown to be a viable method to induce directional ordering, achieve enhanced thermal conductivity, and reduce CTE at relatively low filler loadings [23]. Furthermore, processing approaches favoring basal-plane alignment and interconnected networks, such as external fields, templating or self-assembly processes, may contribute to oriented conductive networks [16,20,23].

Cordierite, also called magnesium aluminium silicate ceramic, is highly valued for its extremely low and sometimes negative coefficient of thermal expansion (CTE). The crystal structure of cordierite contains open rings formed by SiO_4/AlO_4 tetrahedral structures, which results in very low change in dimensions with temperature [24,25]. The theoretical CTE of the cordierite is usually between 0.1 and 2.0 × 10^{-6}/°C. Cordierite can be used as shrinkage compensator in polymeric underfill systems for electronics. Substitution of some parts of the epoxy matrix with cordierite helps to fine-tune the overall composite CTE to better match the silicon dies and organic substrates, reducing the thermomechanical stresses at the interface that cause fatigue and mechanical failure of solder-joints under thermal cycling [24-26]. Moreover, the low CTE of cordierite makes it more resistant to thermal shock, which agrees with the flip-chip packaging requirement to maintain the dimensional stability during the heat-up and cooling off cycles [24,27]. However, to achieve these benefits in practice, it is necessary to control the content of cordierite, microstructure (including phase purity of α-cordierite vs. μ-cordierite), porosity and dispersion in the epoxy matrix carefully, to avoid processing issues such as cracking or high viscosity [24,28].

Numerous studies support the application of cordierite as a low-CTE filler in epoxy composites. These include designs which co-develop cordierite with other ceramic phases (such as mullite) or incorporate cordierite into porous architectures to tailor mechanical performance and thermal expansion. Cordierite's low dielectric constant, chemical durability and favorable high temperature stability all support its use as a functional component in protective coatings and electronic packaging, according to reports. To reduce residual stresses and maximize thermal stability, processing techniques for cordierite-enhanced underfills focus on achieving dense, low-porosity phases with controlled crystallization while maintaining sufficient flow characteristics for capillary underfill processes. Previous research suggests that cordierite can effectively improve the thermomechanical properties of epoxy underfills due to its low coefficient of thermal expansion and excellent thermal shock resistance. However, achieving these benefits depends strongly on the control of formulation parameters, sintering-induced phase development, and microstructural evolution. [25-29].

2. METHODOLOGY

Bisphenol-A epoxy was chosen as a polymer matrix. Hexagonal boron nitride (hBN) nanopowder with an average particle size of 70 nm and cordierite powder with a particle size of 5 μm were incorporated as fillers, whereas diethyltoluenediamine (DETDA) was used as the curing agent.

2.1. Sample Preparation

Samples of epoxy/hexagonal boron nitride (hBN) composite were prepared by gradually adding hBN (70 nm) into an epoxy system at 0, 5, 10, 15 and 20 vol.% loadings. The powders were dispersed into the epoxy matrix by mechanical stirring for 15 min. Ultrasonication for another 15 min was conducted at room temperature to break up particle agglomerates and enhance the distribution of filler particles. DETDA hardener was then added to the mixture at 24 phr and stirred for an additional 10 min. The mixture was then degassed in vacuum for 10-15 minutes before curing to remove the entrapped air and aid to reduce the formation of voids in the specimen. After that, the degassed resin was poured into a mold (100 mm × 100 mm × 3 mm), cured at 100 °C for 12 hours, and post-cured at 120 °C for 5 hours. Epoxy/hBN composite plates with various filler contents were obtained after cooling down to room temperature. To compare the two single-filler systems, epoxy/5 μm cordierite composite was also fabricated using the same vol.% loadings (0–20 vol.%) under the same dispersion, degassing, and curing conditions as that of epoxy/hBN composite described above.

3. DATA COLLECTION AND ANALYSIS

Viscosity, thermal conductivity, dielectric constant, flexural properties and fracture toughness were measured to obtain experimental data to assess the performance of the prepared composites. Rheological properties were analyzed through viscosity measurements, thermal dissipation performance through thermal conductivity measurements, and electrical insulation through dielectric constant measurements. Flexural and fracture toughness tests were conducted to characterize the mechanical resistance of the specimens against deformation and cracking.

3.1. Viscosity Test

The rheological properties of the underfill materials were measured for the processing behavior of the materials using a Brookfield rotational viscometer. The instrument measures the torque required to rotate a spindle at a controlled speed in a sample, which is a measure of the resistance to the flow and internal friction of the material. The measurements were performed according to ASTM D2393 to ensure a standardized and reliable evaluation of the viscosity of the epoxy resin, filler (hBN or cordierite) and curing agent system.

The prepared epoxy mixture was introduced into the measurement chamber for the testing procedure, and the viscometer spindle was immersed in the fluid. Viscosity was measured at different rotational speeds (rpm) to study the effect of shear rate on flow behavior. The results are reported in centipoise (cP), where lower values indicate better flowability. This parameter is especially important for underfill applications, since a sufficiently low viscosity is necessary to allow efficient capillary flow into the narrow gaps between the semiconductor die and the substrate.

3.2. Thermal Conductivity Test

The heat dissipation capability of the formulated underfills was evaluated by measuring their thermal conductivity using a KD2 Pro Thermal Properties Analyzer equipped with an RK-1 sensor. Since the RK-1 probe is designed for solid samples, the epoxy/BN and epoxy/cordierite composites were prepared in the form of rectangular specimens measuring 60 mm × 20 mm × 20 mm. For the measurement, a central hole with a diameter of 4 mm was carefully drilled into each specimen to accommodate the sensor probe and ensure proper contact during the testing process. The thermal conductivity measurements were performed with a fixed sampling interval of 15 s to maintain consistency and improve data reliability throughout the testing process.

3.3. Dielectric Constant Test

The dielectric properties of the composite specimens were characterized using a high-precision impedance analyzer in accordance with ASTM D150. These measurements are important for underfill materials because they must provide reliable electrical insulation while minimizing signal loss in high-frequency semiconductor devices. Measurements were taken at room temperature under controlled ambient conditions of approximately 50% relative humidity using a digital multimeter and a dedicated fixture to determine capacitance and dissipation factor.

For specimen preparation the composites were cast into circular discs of 20 mm diameter and 1 mm thickness. To ensure good electrical contact and minimize interfacial resistance, both faces of each specimen were coated with a thin layer of conductive silver paint before measurement. The dielectric constant was then calculated from the measured capacitance of the sample with respect to that of free space (air) using the following equations:

$$C = \frac{\varepsilon_0 \varepsilon_r A}{d} \quad (1)$$

$$\varepsilon_r = \frac{C \cdot d}{\varepsilon_0 \cdot A} \quad (2)$$

where:

ε_r is the dielectric constant (relative permittivity).

C is the measured capacitance (F).

d is the thickness of the specimen (m).

A is the area of the electrodes (m^2).

ε_0 is the permittivity of free space (8.854×10^{-12} F/m).

3.4. Flexural Test

The flexural properties of the epoxy composites were measured to determine the stiffness and resistance to bending deformation. The test was performed in a three-point bending configuration, in which the specimen is loaded at the midpoint while supported at both ends, generating tensile stress on the outer surface of the beam. The measurements were conducted according to the ASTM D790 using an Instron Universal Testing Machine (Model 5569). Rectangular samples of 60 mm × 12.7 mm × 3 mm were prepared for the testing with a support span of approximately 50 mm. A constant crosshead speed of 2.38 mm/min was used throughout the entire experiment to provide uniform loading conditions.

The flexural strength was calculated using the following equations:

$$\sigma_f = \frac{3PL}{2bd^2} \quad (3)$$

where:

σ_f = midpoint stress (MPa)

P = load at a specified point on the curve of load-deflection (N)

L = support span length (mm)

3.5. Fracture Toughness Test

Fracture toughness is a measure of the ability of a brittle material to resist crack initiation and propagation under an applied stress. It is typically expressed in terms of the critical stress intensity factor (K_{1C}), where higher values indicate greater resistance to fracture and better damage tolerance. In this study, fracture testing was performed using an Instron Universal Testing Machine (Model 5569) in accordance with ASTM D638 standards.

The specimens (60 mm × 12.7 mm × 3 mm) were prepared with an initial 4 mm notch serving as a crack initiator. Testing was performed in the tensile opening mode (Mode I) at a constant crosshead speed of 1 mm/min. The fracture toughness was subsequently determined using the following equation:

$$K_{1C} = \frac{F_{max}\sqrt{\pi a}}{Bw} f\left(\frac{a}{w}\right) \quad (4)$$

$$f\left(\frac{a}{w}\right) = 1.99 - 0.41\left(\frac{a}{w}\right) + 18.7\left(\frac{a}{w}\right)^2 - 38.48\left(\frac{a}{w}\right)^3 + 53.85\left(\frac{a}{w}\right)^4 \quad (5)$$

where,

F_{max}: Maximum force in the force-deflection trace (N)

a: Total notch length (m)

B: Thickness of specimen (m)

w: Width of specimen (m)

$f\left(\frac{a}{w}\right)$: geometric factor near unities that depend on details of specimen geometry.

3.6. Scanning Electron Microscopy

The filler dispersion and the fracture surface morphology of the specimens were analyzed by using a scanning electron microscope (SEM). Fractured surfaces were coated with a thin layer of palladium using a sputter coater before observation to minimize surface charging during imaging. The samples were then mounted on aluminum stubs for analysis. Morphological characterization was performed on a JEOL JSM-6010LV SEM at an accelerating voltage of 10 kV. Once the specimen was vented and all parameters set at a safe clearance distance the specimen was transferred into the chamber. The chamber was then sealed and evacuated to the desired vacuum conditions. The working distance was adjusted to ~20mm in order to get clear and stable micrographs during imaging. Once the analysis was complete the chamber was re-vented prior to sample removal.

4. DISCUSSION AND RESULTS

This section presents an analysis of the experimental results obtained from the single-filler epoxy (EP) systems. The effects of hexagonal boron nitride (hBN) and cordierite (COR) at various volume fractions are examined to understand how filler loading influences the overall material behavior. The trade-off between improved thermal conductivity and higher viscosity is highlighted, as well as the effect of morphology of filler on controlling the mechanical properties, fracture toughness and dielectric properties. The discussion is framed within the requirements of microelectronic packaging to evaluate optimal filler loadings for high-performance underfill applications.

4.1. Viscosity

All epoxy composites [30] exhibit shear thinning, as shown in Figure 1, where viscosity decreases with increasing shear rate. This pseudoplastic behaviour is most pronounced in high-loading formulations, such as EP-COR at 20 vol.% and EP-HBN at 10 vol.%, where the viscosity reduction under shear is significant, enabling flow under

dispensing conditions despite high static viscosity. Consequently, both the COR- and hBN-filled systems become more processable in the high-shear environment of jetting or capillary flow, in line with the underfill processing targets [31]. This shear-thinning phenomenon is attributed to the structural disruption of the composite matrix; at low shear rates, the fillers form a linked network that resists flow, and the polymer chains are tightly entangled. At high large shear rates, the hydrodynamic forces break down the weak, secondary filler-filler physical networks, entangle and orient the epoxy molecular chains along the flow direction, lowering flow resistance [32].

Compared to cordierite, the hBN-filled systems exhibit a greater degree of shear thinning. With increasing shear, EP-HBN10 exhibits a significant viscosity reduction (from high rest viscosity to much lower values), suggesting that plate-like hBN networks are extremely vulnerable to shear-induced breakdown. In contrast, cordierite, although still thinning, exhibits a relatively milder response because of its more isotropic morphology. This difference highlights the role of filler shape in modulating the effective processing window and the dispensed flow in high-shear dispensing, with hBN providing more thermal benefits at the expense of stronger shear-thinning behaviour [33,34].

From a processing perspective, these shear-thinning trends suggest that dispensing parameters should be optimized to enhance high-shear flow and limit low-shear penalties, especially for hBN-rich formulations that can potentially restrict capillary flow at rest. To ensure reliable underfill infiltration through tight gaps without voids, the results favor the use of COR-rich or hybrid COR–hBN approaches to balance flowability with thermal performance, tuning jetting pressures, nozzle dwell times, and shear regimes [33,35]. This approach seeks improved thermal management by controlling the hBN content and dispersion while leveraging the favorable shear-thinning tendency to achieve realistic fill.

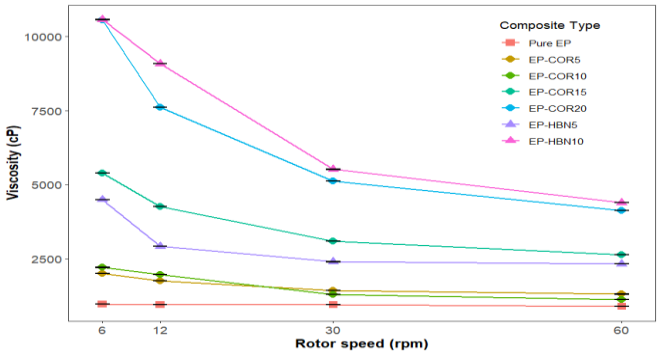

Figure 1. Viscosity trends for EP-HBN and EP-COR at various filler loadings and rotor speeds.

4.2. Thermal Conductivity

Figure 2 shows the effect of increased filler volume percentage on the thermal conductivity of epoxy composites with hexagonal boron nitride and cordierite fillers. The matrix reveals a starting thermal conductivity of ~0.24 W/mK with a loading of 0 vol.%. The thermal performance shows an obvious increasing trend when both fillers are at 20 vol.%. This improvement is due to the replacement of particles with higher intrinsic thermal conductivity than low conductivity polymer matrix which is an important requirement for microelectronic underfill applications [17,36].

The two types of filler exhibit significantly different performance. The hBN composite shows a greater rate of enhancement, reaching a thermal conductivity of ~1.05 W/mK at 20 vol.%. In comparison, the cordierite composite only reaches 0.46 W/mK at the same volume percentage [35,36]. This substantial difference indicates that hBN is more than twice as effective as COR in augmenting the heat transport through the system [36,37].

The exponential growth of the hBN curve, particularly between 15 vol.% and 20 vol.% loading, indicates the phenomenon of thermal percolation threshold. This value represents the percolation threshold for the transition of the filler particles from discrete clusters to a continuous percolated network across the matrix. These "thermal bridges" allow heat-carrying phonons to flow via high-conductivity channels and circumvent the high-resistance polymer matrix. The relatively poor performance of COR at low loading indicates a higher percolation threshold or a less favorable particle shape [15,17,38]. Thus, hBN is a better candidate to create thermal conductive networks to enhance heat dissipation.

The thermal conductivity of the hBN composite increases immediately at 5 vol.% as seen in Figure 2, while the thermal conductivity of the COR composite marginally decreases below the baseline of the pure epoxy. The reasons for a composite to have a worse thermal conductivity than the base resin at low loadings are mostly due to the creation of micro-voids during the mixing process and interfacial thermal resistance. At these low concentrations the filler particles exist as distinct islands that heat must flow through as they are too far apart to form a linked “thermal highway” [15,16,39].

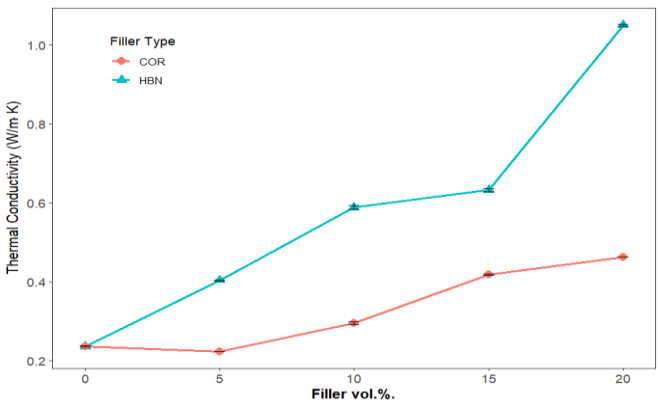

Figure 2. Thermal conductivity of EP-hBN and EP-COR at various filler loadings.

4.3. Dielectric Constant

The results of the dielectric constant show that the fillers added to epoxy underfill improve the dielectric response in a near linear fashion with filler content from a baseline of about 5.07 for neat epoxy. The dielectric constant increases with the volume fraction for both the COR and hBN composites, in agreement with the Rule of Mixtures, which stipulates that the overall permittivity is given by the sum of the filler and matrix contributions [40,41]. At 10 vol%, the COR-filled epoxy is lower (~5.21) than that of the hBN-filled epoxy (~5.60), indicating higher interfacial polarisation and the intrinsically larger dielectric constant of hBN, especially at higher surface areas and with Maxwell-Wagner-Sillars effects at work at the interfaces [36,41].

For applications, the larger dielectric constant of hBN composites implies an increased capacity for capacitive energy storage, but this is also a trade-off for high frequency underfill where a low dielectric constant is required to prevent crosstalk and signal delay. Moreover, the overall better flow behaviour of COR at similar loadings makes cordierite-filled systems milder dielectric rise, therefore better satisfying the signal integrity requirements while keeping a more advantageous processing rheology [41,42]. Epoxy nanocomposites can be further modified in their dielectric performance by filler surface treatment and coupling through the effect on interfacial polarisation and overall permittivity [36,42].

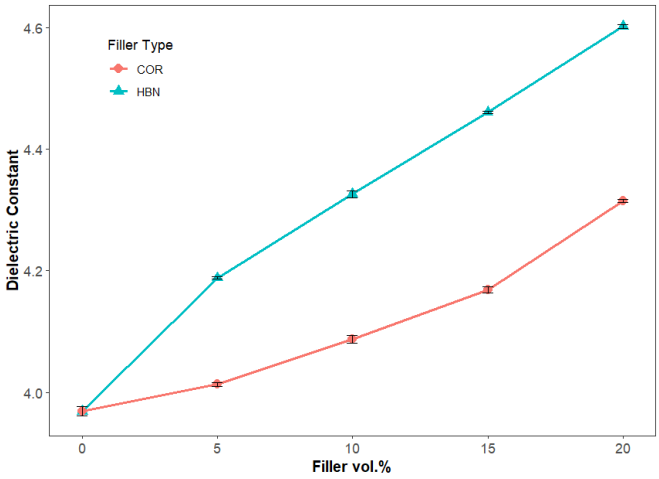

Figure 3. Dielectric constants of hBN and COR filled epoxy composites at various filler loadings.

4.4. Flexural Strength

In the systems with COR and hBN-filled epoxy, the flexural strength falls gradually with the increase of filler concentration. This pattern agrees with the general trade-off for heavily filled thermosets, where filler-matrix interfaces and possible particle agglomeration operate as stress concentrators weakening the composite. The clean epoxy presents an initial flexural strength of around 145 MPa, which decreases considerably with increasing volume fraction, especially at higher loadings [36,40].

The strength drop of the hBN-filled composites is more pronounced than that of the COR systems. This behaviour is linked to the platelet-like morphology of hBN, which can provide favourable planes for crack propagation, and to a higher sensitivity to the interfacial bonding quality when surface treatment is insufficient. In contrast, the more isotropic geometry of the cordierite particles tends to promote a more uniform stress distribution within the matrix, enabling the composites to maintain strengths more than ~120 MPa up to 10 vol% loading [36,40].

At larger filler amounts (20 vol.%) both systems show a significant decrease in mechanical performance, with hBN composites decreasing to ~60 MPa. These results highlight the natural processing–performance trade-off: cordierite gives higher mechanical stability with little thermal enhancement, whereas hBN increases thermal performance at the expense of mechanical integrity.

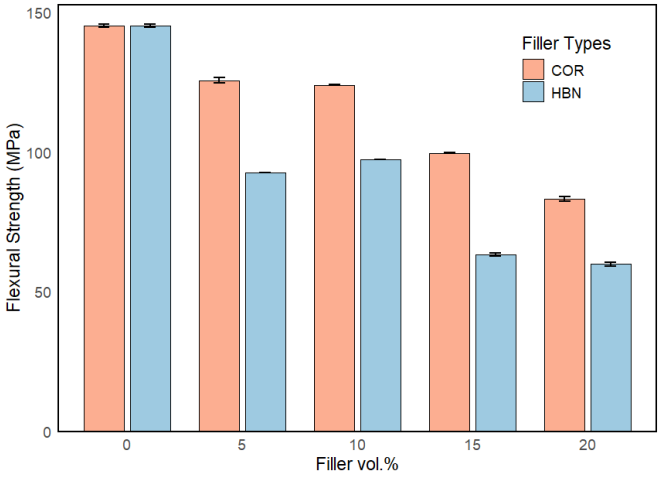

Figure 4. Flexural strength of EP-hBN and EP-COR at various filler loadings.

4.5. Fracture Toughness

The fracture toughness (K 1C) of the two systems, cordierite (COR) and hBN filled epoxy, reveals a non-monotonic dependence on filler loading. The neat epoxy exhibits an initial value of about 6.6 MPa·m$^{1/2}$, however there is a steep drop at 5 vol.% filler. Then a peak at 10 vol.% was recorded and thereafter the fracture toughness decreased with additional filler addition. This behaviour suggests a change in the dominant failure mechanism: at lower filler content (5 vol.%) the particles mainly act as stress concentrators promoting crack initiation, while at intermediate loading (10 vol.%) they start to contribute to the crack resistance through mechanisms such as crack pinning and crack deflection [24].

The fracture toughness of cordierite-filled composites is higher than that of hBN-filled systems across all loading levels. At 10 vol.%, the COR system reaches ~5.7 MPa·m$^{1/2}$, almost recovering the toughness of the neat epoxy, whereas the hBN system only reaches ~2.8 MPa·m$^{1/2}$. This difference can be explained by the poorer interfacial

bonding and the intrinsic anisotropic platelet nature of hBN. The poor interfacial bonding facilitates localised debonding at the filler–matrix interface, as the relatively smooth, unfunctionalized surfaces of hBN platelets do not interact well with the crosslinked epoxy network. When the propagating crack finds these interfaces, it tends to propagate along the weak borders rather than be deflected, leading to the premature failure [43].

At higher loadings (15–20 vol.%), filler agglomeration further aggravates this behaviour by generating resin-deficient zones that serve as easy routes for crack propagation, contributing to the observed drop in toughness beyond the 10 vol.% peak. Overall, our results suggest a specific processing-property trade-off: cordierite gives greater mechanical stability with mild reinforcing effects, while hBN provides enhanced thermal and dielectric performance at the expense of lower fracture resistance at larger filler percentages.

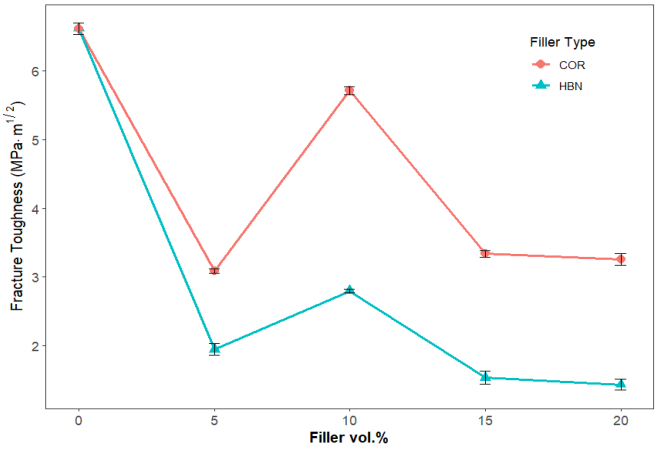

Figure 5. Fracture toughness of hBN and COR filled epoxy composites at various filler loadings.

4.6. Scanning Electron Microscopy

The fracture surface of the neat epoxy is shown in Figure 6(a). It exhibits a highly shattered glassy appearance with pronounced river-like patterns, which is characteristic of brittle failure in heavily crosslinked thermosetting polymers. In the absence of any reinforcing filler particles, the propagating fracture encounters negligible resistance and propagates along the zones of localized high stress. This leads to rapid and unstable spread of cracks in the whole matrix with low plastic deformation or energy dissipation [44]. This intrinsically brittle fracture is used as a baseline to assess the toughening effects introduced in the filled composite systems.

The SEM micrograph of the fracture surface of the 10 vol.% hBN composites shows a very rough and textured surface as shown in Figure 6(b). This morphology suggests that the matrix resin obstructs the effective stress transfer that is responsible for the creation of very tortuous crack propagation paths [17,38]. The formation of microstructural packing flaws is seen to be more significant beyond the 10 vol.% threshold directly contributing to the observed decrease in fracture toughness. Contrary to the smooth morphology of the virgin matrix, hBN-filled composites show a much rougher fracture surface with a good dispersion of platelets across the crosslinked network without any noticeable large-scale aggregation [46].

The SEM image of 20 vol.% hBN filled epoxy composite (Figure 6(c)) presents a multi-planar fractured surface which is highly uneven and excessively rough. At this maximal filler loading, the high density of interconnected hBN platelets seen throughout the matrix illustrates the successful formation of highly dense routes for thermal networks. But the surface also reveals more microstructural packing flaws and isolated areas of dense filler accumulation. Despite the high aspect ratio of hBN platelets, which nonetheless induce significant crack deflection and branching, the crack courses are severely disturbed, indicating that localised resin-poor patches and weak interfacial barriers between surrounding platelets create a high density of micro gaps. This structural pattern accounts for the drop in KIC at 20 vol.%, since the benefits of the toughening mechanisms are negated by structural defects and insufficient interfacial stress transmission [17,45].

The SEM picture of the epoxy composite filled with 10% COR is given in Fig. 6(d). At this intermediate loading, the cordierite particles are very well distributed throughout the matrix, with low agglomeration and good particle-matrix wetting. The presence of multiple multiplanar steps, localised microcracks, and discrete shear bands around the embedded inclusions indicates a significant disturbance in the crack-front advancement. The highly textured surface [17,45,46] suggests that the cordierite particles acted as effective structural barriers, leading to the deflection and pinning of the progressing crack point. The efficient triggering of energy dissipation processes directly explains the ability of the composite to almost totally restore its initial toughness at this optimal loading concentration.

Figure 6(e) shows SEM picture for epoxy composite with 20 vol.% COR filler. The high packing density of the inclusions leads to an exponential increase in the filler-matrix interfacial area as the filler loading climbs to 20 vol.%. This high boundary density keeps strong interfacial polarization (Maxwell-Wagner-Sillars effect), in which charge carriers pile up at phase borders under an electric field to give the apparent rise in the dielectric constant [17,38,46]. The cordierite clusters still offer good crack deflection and propagation resistance, but the tight packing of the clusters leaves resin-poor borders between adjacent particles. The absence of matrix resin prevents the efficient transfer of stress along the very sinuous fracture paths [17,38]. The microstructural imbalance increases with the filler content over the threshold of 10 vol.% and results in a decrease of mechanical performance. Packing flaws break the integrity of the composite network and are associated with the observed decrease of both flexural strength and fracture toughness.

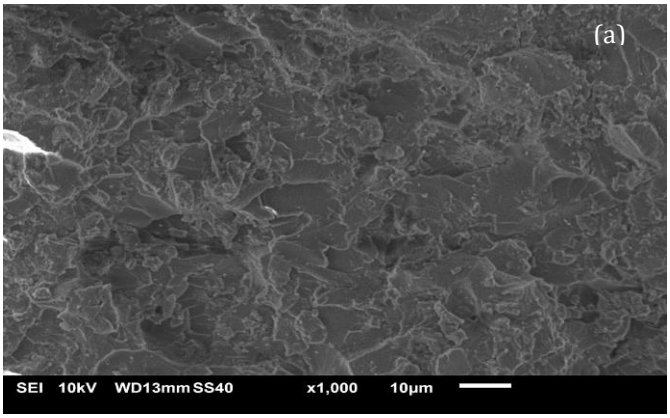

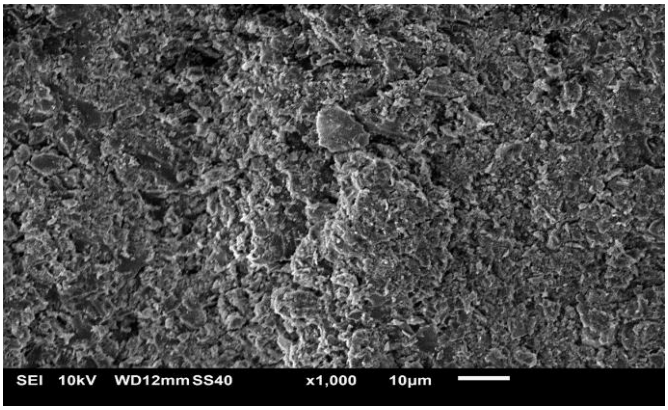

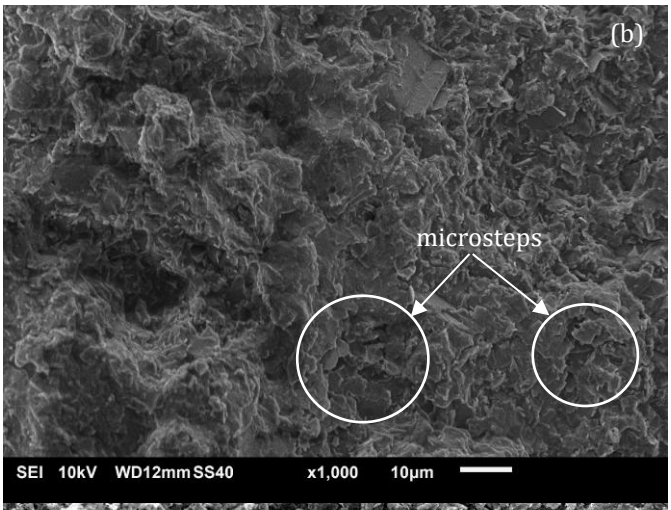

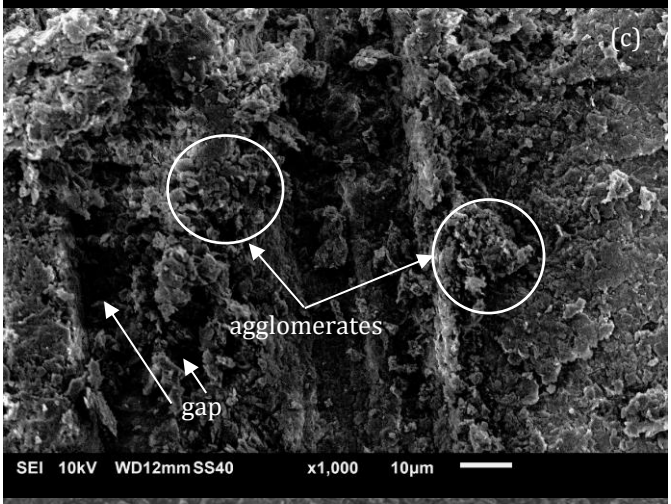

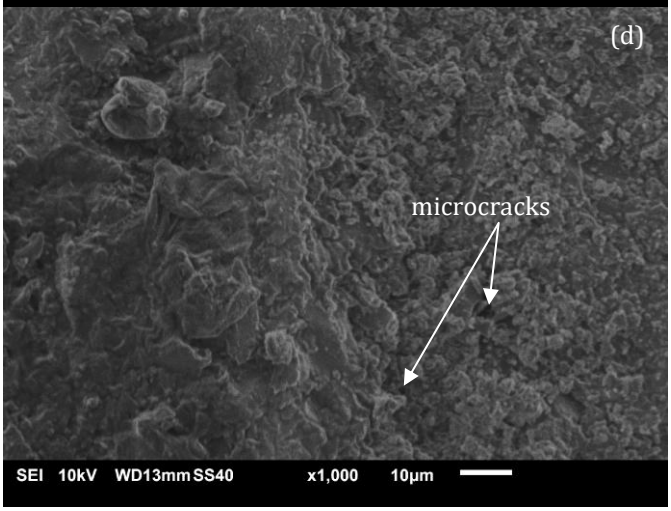

Figure 6. SEM micrographs of: (a) pure epoxy, (b) 10 vol.% hBn filled epoxy, (c) 20 vol.% hBn filled epoxy, (d) 10 vol.% Cor filled epoxy, (e) 20 vol.% Cor filled epoxy.

5. CONCLUSION

The effects of hexagonal boron nitride (hBN) and cordierite (COR) as single fillers in epoxy underfill systems for microelectronic packaging applications were investigated in this work. The results showed that both fillers affected the thermal, rheological, dielectric and mechanical properties of the epoxy matrix. However, their impacts were rather different due to their different particle characteristics.

The addition of hBN resulted in a more significant improvement of heat conductivity than cordierite. The hBN-filled composite with 20 vol.% loading had a thermal conductivity of 1.05 W/mK. The similar system filled with cordierite had a value of 0.46 W/mK. The improved performance of hBN is due to the development of thermally conductive channels in the epoxy matrix. However, the increase in thermal conductivity was associated with an increase in viscosity, an increase in dielectric constant and a decrease in mechanical performance at high filler loadings.

The composites with cordierite filling had relatively low thermal conductivity but superior retention of flexural strength and fracture toughness. Furthermore, the dielectric constant showed less rise with filler loading. Cordierite was a promising choice for applications where increased signal integrity and dimensional stability are required. Additional SEM investigations showed that properly scattered cordierite particles effectively prevented crack progression especially at moderate filler concentrations.

Among the studied compositions, the one with 10 vol.% filler loading gave the best overall balance of properties. Both filler systems displayed good processability and reasonable mechanical characteristics at this loading level. The maximum fracture toughness was achieved at 10 vol.% filler loading, demonstrating the prevalence of crack deflection and energy dissipation mechanisms before particle agglomeration and filler-induced defects at higher concentrations.

In summary, hBN is more suited to situations where heat control is the major requirement, while cordierite gives advantages in mechanical dependability and dielectric performance. The results obtained in this work are a useful reference for the design of epoxy underfill materials and a basis for future investigations using hybrid hBN-cordierite filler systems in order to find a more balanced mix of thermal, mechanical and electrical properties.

ACKNOWLEDGMENTS

This material is based upon work supported by Intel Corporation under the funding award of the Advanced Packaging Research Grant 2024 cycle.

REFERENCES

[1] Y. Wen, C. Chen, Y. Ye, Z. Xue, H. Liu, X. Zhou, Y. Zhang, et al., "Advances on Thermally Conductive Epoxy-Based Composites as Electronic Packaging Underfill Materials—A Review," *Adv. Mater.*, vol. 34, no. 52, 2022, Art. no. 2201023. doi: 10.1002/adma.202201023.

[2] T. Li, P. Li, R. Sun, and S. Yu, "Polymer-based nanocomposites in semiconductor packaging," *IET Nanodielectrics*, vol. 6, no. 3, pp. 147-158, 2023. doi: 10.1049/nde2.12050.

[3] Z. Plachý, A. Pražanová, K. Dušek, and A. Géczy, "Underfill: A Review of Reliability Improvement Methods in Electronics Production," *Polymers*, vol. 17, no. 16, 2025, Art. no. 2206. doi: 10.3390/polym17162206.

[4] Z. Zhang, H. Li, and C. P. Wong, "Novel Reworkable Fluxing Underfill for Board-Level Assembly," *IEEE Trans. Adv. Packag.*, vol. 27, no. 3, pp. 525-532, Aug. 2004. doi: 10.1109/tadvp.2004.831836.

[5] C.-C. Tuan, N. J. Pataki, Z. Lin, Y. Chen, Y. Liu, K.-S. Moon, Z. Li, et al., "Self-Patterning of Silica/Epoxy Nanocomposite Underfill by Tailored Hydrophilic-Superhydrophobic Surfaces for 3D Integrated Circuit (IC) Stacking," *ACS Appl. Mater. Interfaces*, vol. 9, no. 10, pp. 8437-8442, 2017. doi: 10.1021/acsami.6b15771.

[6] C. Chen, H. Wang, X. Yang, Z. Xue, H.-Y. Liu, X. Xie, and Y.-W. Mai, "Structure, rheological, thermal conductive and electrical insulating properties of high-performance hybrid epoxy/nanosilica/AgNWs nanocomposites," *Compos. Sci. Technol.*, vol. 128, pp. 207-214, 2016. doi: 10.1016/j.compscitech.2016.04.005.

[7] E. Suhir and R. Ghaffarian, "Flip-Chip (FC) and Fine-Pitch-Ball-Grid-Array (FPBGA) Underfills for Application in Aerospace Electronics—Brief Review," *Aerospace*, vol. 5, no. 3, 2018, Art. no. 74. doi: 10.3390/aerospace5030074.

[8] I. Lorero, A. Mujica, M. Campo, and S. G. Prolongo, "Mechanical recycling and electro-thermal welding of epoxy vitrimer nanocomposites," *Polym. Compos.*, vol. 45, no. 7, pp. 6041-6058, 2024. doi: 10.1002/pc.28178.

[9] M. Seidlová, J. Hodul, N. Žižková, and R. P. Borg, "Possibilities of Influencing the Crystallization Process of Bisphenol A- and Bisphenol F-Based Epoxy Resins Used for Hydrophobic Coatings on Concrete," *Polymers*, vol. 15, no. 19, 2023, Art. no. 3871. doi: 10.3390/polym15193871.

[10] B. Francis, S. Thomas, R. Sadhana, N. Thuaud, R. Ramaswamy, S. Jose, and V. L. Rao, "Diglycidyl ether of bisphenol-A epoxy resin modified using poly(ether ether ketone) with pendent tert-butyl groups," *J. Polym. Sci. B Polym. Phys.*, vol. 45, no. 17, pp. 2481-2496, 2007. doi: 10.1002/polb.21238.

[11] K. Fu, Q. Xie, F. Lü, Q. Duan, X. Wang, Q.-S. Zhu, and Z. Huang, "Molecular Dynamics Simulation and Experimental Studies on the Thermomechanical Properties of Epoxy Resin with Different Anhydride Curing Agents," *Polymers*, vol. 11, no. 6, 2019, Art. no. 975. doi: 10.3390/polym11060975.

[12] X. Wang, W. Li, Z. Zhang, K. Chen, and W. Gan, "Selective localization of multi-walled carbon nanotubes in epoxy/polyetherimide system and properties of the conductive composites," *J. Appl. Polym. Sci.*, vol. 136, no. 35, 2019, Art. no. 47911. doi: 10.1002/app.47911.

[13] I. Işık-Gülsaç, Ü. Yilmazer, and G. Bayram, "Effects of mixing sequence on epoxy/polyether polyol/organoclay ternary nanocomposites," *Plast. Rubber Compos.*, vol. 49, no. 8, pp. 368-377, 2020. doi: 10.1080/14658011.2020.1763661.

[14] W. Zhang, H. Li, L. Gao, Q. Zhang, W.-H. Zhong, G. Sui, and X. Yang, "Molecular simulation and experimental analysis on thermal and mechanical properties of carbon nanotube/epoxy resin composites with different curing agents at high-low temperature," *Polym. Compos.*, vol. 39, no. S2, 2017. doi: 10.1002/pc.24352.

[15] S. Ghaffari-Mosanenzadeh, O. A. Tafreshi, E. Dammen-Brower, E. Rad, M. Meysami, and H. E. Naguib, "A review on high thermally conductive polymeric composites," *Polym. Compos.*, vol. 43, no. 2, pp. 692-711, 2021. doi: 10.1002/pc.26420.

[16] S. Yu, X. Shen, and J.-K. Kim, "Beyond homogeneous dispersion: oriented conductive fillers for high-κ nanocomposites," *Mater. Horizons*, vol. 8, no. 11, pp. 3009-3042, 2021. doi: 10.1039/d1mh00907a.

[17] M. Dong, H. Zhang, L. Tzounis, G. Santagiuliana, E. Bilotti, and D. G. Papageorgiou, "Multifunctional epoxy nanocomposites reinforced by two-dimensional materials: A review," *Carbon*, vol. 185, pp. 57-81, 2021. doi: 10.1016/j.carbon.2021.09.009.

[18] Y. Tominaga, "Review on powder technologies for hexagonal boron nitride/polymer composites with high thermal conductivities," *J. Ceram. Soc. Jpn.*, vol. 131, no. 11, pp. 863-869, 2023. doi: 10.2109/jcersj2.23109.

[19] H. Hong, J. Kim, and T.-I. Kim, "Effective Assembly of Nano-Ceramic Materials for High and Anisotropic Thermal Conductivity in a Polymer Composite," *Polymers*, vol. 9, no. 9, 2017, Art. no. 413. doi: 10.3390/polym9090413.

[20] Z. Cai, N. Thirunavukkarasu, X. Diao, H. Wang, L. Wu, C. Zhang, and J. Wang, "Progress of Polymer-Based Thermally Conductive Materials by Fused Filament Fabrication: A Comprehensive Review," *Polymers*, vol. 14, no. 20, 2022, Art. no. 4297. doi: 10.3390/polym14204297.

[21] M. M. Hossain, Y.-K. Kim, H. Lim, I. J. Lim, Y. Joo, H.-D. Jeong, J. H. Kim, et al., "Highly Interconnected Thermal Conduction Highway for Highly Thermally Conductive and Mechanically Strong Polymeric Composites," *ACS Appl. Mater. Interfaces*, vol. 16, no. 47, pp. 65307-65318, 2024. doi: 10.1021/acsami.4c13986.

[22] I. Isarn, F. Ferrando, À. Serra, and C. Urbina, "Novel BN-epoxy/anhydride composites with enhanced thermal conductivity," *Polym. Adv. Technol.*, vol. 32, no. 4, pp. 1485-1492, 2020. doi: 10.1002/pat.5184.

[23] Z. Lin, Y. Liu, S. Raghavan, K.-S. Moon, S. K. Sitaraman, and C.-P. Wong, "Magnetic Alignment of Hexagonal Boron Nitride Platelets in Polymer Matrix: Toward High Performance Anisotropic Polymer Composites for Electronic Encapsulation," *ACS Appl. Mater. Interfaces*, vol. 5, no. 15, pp. 7633-7640, 2013. doi: 10.1021/am401939z.

[24] A. Shyam, E. Lara-Curzio, A. Pandey, T. R. Watkins, and K. L. More, "The Thermal Expansion, Elastic and Fracture Properties of Porous Cordierite at Elevated Temperatures," *J. Am. Ceram. Soc.*, vol. 95, no. 5, pp. 1682-1691, 2012. doi: 10.1111/j.1551-2916.2012.05125.x.

[25] I. P. de Brito, E. P. de Almeida, G. de Araújo Neves, H. de Lucena Lira, R. R. Menezes, V. J. da Silva, and L. N. de Lima Santana, "Development of cordierite/mullite composites using industrial wastes," *Int. J. Appl. Ceram. Technol.*, vol. 18, no. 1, pp. 253-261, 2020. doi: 10.1111/ijac.13622.

[26] H. Cheng, F. Ye, Jun Chang, and S.-Z. Wu, "In situ synthesis and thermal shock resistance of a cordierite-mullite composite for solar thermal storage," *Int. J. Appl. Ceram. Technol.*, vol. 16, no. 2, pp. 772-780, 2018. doi: 10.1111/ijac.13135.

[27] M. E. Miller and S. T. Misture, "Stoichiometric (Ni,Mg)-Cordierite Glass–Ceramics," *J. Am. Ceram. Soc.*, vol. 93, no. 4, pp. 1018-1025, 2010. doi: 10.1111/j.1551-2916.2009.03534.x.

[28] K. K. Eing, B. Johar, L.-N. Ho, and Y. Zabar, "Influence of Sintering Temperature on Crystallization Behavior of Cordierite synthesized from Non-Stoichiometric Formulation," *MATEC Web Conf.*, vol. 78, 2016, Art. no. 01099. doi: 10.1051/matecconf/20167801099.

[29] Y. Yang, J. Yan, S. Cheng, G. Liu, B. Chen, K. Zheng, L. Chen, et al., "Formation, conversion, and elimination of intermediate spinel phase in MgO/kaolin mixture firing for cordierite," *Int. J. Appl. Ceram. Technol.*, vol. 21, no. 2, pp. 829-843, 2023. doi: 10.1111/ijac.14550.

[30] W. N. F. Wan Hamad, P.L. Teh, and C. K. Yeoh, "Effect of Acetic Acid as Catalyst on the Properties of Epoxy Foam", *Polym-Plast Technol*. vol. 52, no. 8, pp. 2727-2736, 2013. doi.org/10.1080/03602559.2012.762375

[31] M. Albozahid, H. Z. Naji, Z. K. Alobad, J. K. Wychowaniec, and A. Saiani, "Synthesis and characterization of hard copolymer polyurethane/functionalized graphene nanocomposites: Investigation of morphology, thermal stability, and rheological properties," *J. Appl. Polym. Sci.*, vol. 139, no. 45, 2022. doi: 10.1002/app.53118.

[32] Y. Liu and A. Wilkinson, "Rheological percolation behaviour and fracture properties of nanocomposites of MWCNTs and a highly crosslinked aerospace-grade epoxy resin system," *Compos. Part A Appl. Sci. Manuf.*, vol. 105, pp. 97–107, 2018. doi: 10.1016/j.compositesa.2017.11.012.

[33] A. Kurz, J. Bauer, and M. H. Wagner, "Piezo-Plunger Jetting Technology: An Experimental Study on Jetting Characteristics of Filled Epoxy Polymers," *Fluids*, vol. 4, no. 1, 2019, Art. no. 23. doi: 10.3390/fluids4010023.

[34] M. H. Zamani and Z. Ounaies, "Advancing the 3D printing of magnetoactive epoxy shape memory composites: correlating the rheology, printability, and shape fidelity," Research Square preprint, 2024. doi: 10.21203/rs.3.rs-5449807/v1.

[35] L. Yang, C. K. King, and J. B. Bernstein, "Liquid dispensing encapsulation in semiconductor packaging," *Microelectron. Int.*, vol. 20, no. 3, pp. 29-35, 2003. doi: 10.1108/13565360310487927.

[36] A. Agrawal and S. Chandraker, "An experimental investigation of epoxy-based hybrid composites with hexagonal boron nitride and short sisal fiber as reinforcement for high performance microelectronic applications," *Polym. Eng. Sci.*, vol. 62, no. 1, pp. 160-173, 2021. doi: 10.1002/pen.25841.

[37] Z. Liu, J. Li, and X. Liu, "Novel Functionalized BN Nanosheets/Epoxy Composites with Advanced Thermal Conductivity and Mechanical Properties," *ACS Appl. Mater. Interfaces*, vol. 12, no. 5, pp. 6503–6515, 2020. doi: 10.1021/acsami.9b21467.

[38] G. M. Pinto, J. M. de O. Cremonezzi, H. Ribeiro, R. J. E. Andrade, N. R. Demarquette, and G. J. M. Fechine, "From two-dimensional materials to polymer nanocomposites with emerging multifunctional applications: A critical review," *Polym. Compos.*, vol. 44, no. 3, pp. 1438–1470, 2023. doi: 10.1002/pc.27213.

[39] H. Zhan, "Thermal Transport in 3D Nanostructures," *Adv. Funct. Mater.*, vol. 30, no. 8, 2019, Art. no. 1903841. doi: 10.1002/adfm.201903841.

[40] J. J. Varughese and M. Sreekanth, "Investigation on enhancement of filler dispersion and prediction of mechanical behavior of hexagonal boron nitride/epoxy nanocomposites through machine learning and deep learning models," *Polym. Compos.*, vol. 45, no. 7, pp. 6287-6304, 2024. doi: 10.1002/pc.28197.

[41] W. Zhou, J. Zuo, X. Zhang, and A. Zhou, "Thermal, electrical, and mechanical properties of hexagonal boron nitride–reinforced epoxy composites," *J.*

Compos. Mater., vol. 48, no. 20, pp. 2517-2526, 2013. doi: 10.1177/0021998313499953.

[42] I. A. Tsekmes, P. H. F. Morshuis, J. J. Smit, and R. Kochetov, "The influence of interfaces and water uptake on the dielectric response of epoxy-cubic boron nitride composites," *J. Mater. Sci.*, vol. 50, no. 11, pp. 3929-3941, 2015. doi: 10.1007/s10853-015-8940-1.

[43] M. Li, S.-R. Han, C. Dan, et al., "Boron Nitride-Polymer Composites with High Thermal Conductivity: Preparation, Functionalization Strategy and Innovative Structural Regulation," *Small*, vol. 21, no. 20, 2025, Art. no. 2412447. doi: 10.1002/smll.202412447.

[44] J. H. J. Koay, P. L. Teh, C. K. Yeoh, et al., "The Performance of Hexagonal Boron Nitride (hBN) and Cordierite: Hybrid Filler System in Epoxy Underfill Materials," *Mater. Res. Express*, vol. 13, no. 3, 2026, Art. no. 036301. doi: 10.1088/2053-1591/ae3bb3.

[45] Y. S. Rao, S. Basavannadevaru, N. M. Subbarao, and N. Shetty, "Influence of hBN and MoS2 fillers on toughness and thermal stability of carbon fabric-epoxy composites," *Frat. Ed Integrità Strutt.*, vol. 16, no. 62, pp. 240–260, 2022. doi: 10.3221/igf-esis.62.17.

[46] Z. G. Hernández, O. Molina-Ramírez, J. E. Rivera-Salinas, I. Sifuentes-Nieves, P. González-Morones, and E. Hernández-Hernández, "Boron nitride: The key material in polymer composites for electromobility," *Polym. Compos.*, vol. 46, no. 3, pp. 1976–2029, 2024. doi: 10.1002/pc.29106.